http://sure.sunderland.ac.uk/policies.html or alternatively contact sure@sunderland.ac.uk.

PHILOSOPHICAL TRANSACTIONS B

rstb.royalsocietypublishing.org

Research

Cite this article: Lecointre B *et al*. 2018 Isoform-selective HDAC1/6/8 inhibitors with an imidazo-ketopiperazine cap containing stereochemical diversity. *Phil. Trans. R. Soc. B* **373**: 20170364.
http://dx.doi.org/10.1098/rstb.2017.0364

Accepted: 8 March 2018

One contribution of 18 to a discussion meeting issue 'Frontiers in epigenetic chemical biology'.

Subject Areas:
biochemistry, cellular biology, health and disease and epidemiology, molecular biology

Keywords:
zinc metalloenzymes, epigenetics, histone deacetylases, enzyme inhibitors, peptidomimetics

Author for correspondence:
A. Ganesan
e-mail: a.ganesan@uea.ac.uk

†Present address: CEM SAS, Domaine Technologique de Saclay, Immeuble Ariane, 4 Rue René Razel, 91400 Saclay, France.
‡Present address: ProQinase Breisacher Strasse 117, 79106 Freiburg, Germany.
¶Present address: Loschmidt Laboratories, Department of Experimental Biology and RECETOX, Faculty of Science, Masaryk University, Kamenice 5/A13, 625 00 Brno, Czech Republic.

Electronic supplementary material is available online at https://dx.doi.org/10.6084/m9.figshare.c.4032565.

THE ROYAL SOCIETY PUBLISHING

Isoform-selective HDAC1/6/8 inhibitors with an imidazo-ketopiperazine cap containing stereochemical diversity

Bertrand Lecointre[1,†], Remy Narozny[2], Maria Teresa Borrello[3], Johanna Senger[4], Alokta Chakrabarti[4,‡], Manfred Jung[4], Martin Marek[5,¶], Christophe Romier[5], Jelena Melesina[6], Wolfgang Sippl[6], Laurent Bischoff[1] and A. Ganesan[2]

[1]Normandie University, INSA Rouen, UNIROUEN, CNRS, COBRA (UMR 6014), 76000 Rouen, France
[2]School of Pharmacy, University of East Anglia, Norwich NR4 7TJ, UK
[3]INSERM U1068 Cellular Stress Group, Cancer Research Center of Marseille, Parc scientifique de Luminy, 163 avenue de Luminy, 13288 Marseille Cedex 9, France
[4]Institut für Pharmazeutische Wissenschaften, Albert-Ludwigs-Universität Freiburg, Albertstraße 25, Freiburg 79104, Germany
[5]Département de Biologie Structurale Intégrative, Institut de Génétique et Biologie Moléculaire et Cellulaire (IGBMC), Université de Strasbourg, CNRS, INSERM, 1 rue Laurent Fries, 67404 Illkirch Cedex, France
[6]Institute of Pharmacy, Martin-Luther University of Halle-Wittenberg, 06120 Halle/Saale, Germany

MJ, 0000-0002-6361-7716; AG, 0000-0003-4862-7999

A series of hydroxamic acids linked by different lengths to a chiral imidazo-ketopiperazine scaffold were synthesized. The compounds with linker lengths of 6 and 7 carbon atoms were the most potent in histone deacetylase (HDAC) inhibition, and were specific submicromolar inhibitors of the HDAC1, HDAC6 and HDAC8 isoforms. A docking model for the binding mode predicts binding of the hydroxamic acid to the active site zinc cation and additional interactions between the imidazo-ketopiperazine and the enzyme rim. The compounds were micromolar inhibitors of the MV4-11, THP-1 and U937 cancer cell lines. Increased levels of histone H3 and tubulin acetylation support a cellular mechanism of action through HDAC inhibition.

This article is part of a discussion meeting issue 'Frontiers in epigenetic chemical biology'.

1. Introduction

The zinc-dependent histone deacetylases (HDACs) are a major target for epigenetic drug discovery, with five HDAC inhibitors approved for the treatment of haematological cancers [1,2]. These drugs (figure 1), as well as others in clinical development, share a common pharmacophore composed of a zinc-binding group and a cap connected by a linker [3]. The first approved HDAC inhibitor vorinostat features a hydroxamic acid, and indeed this bidentate chelating functionality remains the most popular choice for the zinc-binding group [4]. Although alternatives such as sulfonamides and carboxylic acids are successful zinc-binding groups against other enzyme targets, they have seldom yielded HDAC inhibitors with submicromolar levels of activity [5]. A rare exception is the marine natural product azumamide E [6,7]. Azumamide E, like the clinically approved drug romidepsin and other macrocyclic peptide or depsipeptide natural product HDAC inhibitors, contain relatively weak monodentate zinc-binding groups such as carboxylic acids, thiols and ketones. Nevertheless, these compounds often bind to the HDAC enzymes with higher affinity than synthetic hydroxamic acids due to the additional binding interactions between the macrocyclic cap and the enzyme rim [8–10]. Furthermore, the size of the macrocycle facilitates discrimination between the 11 human HDAC isoforms. While vorinostat is a pan-HDAC

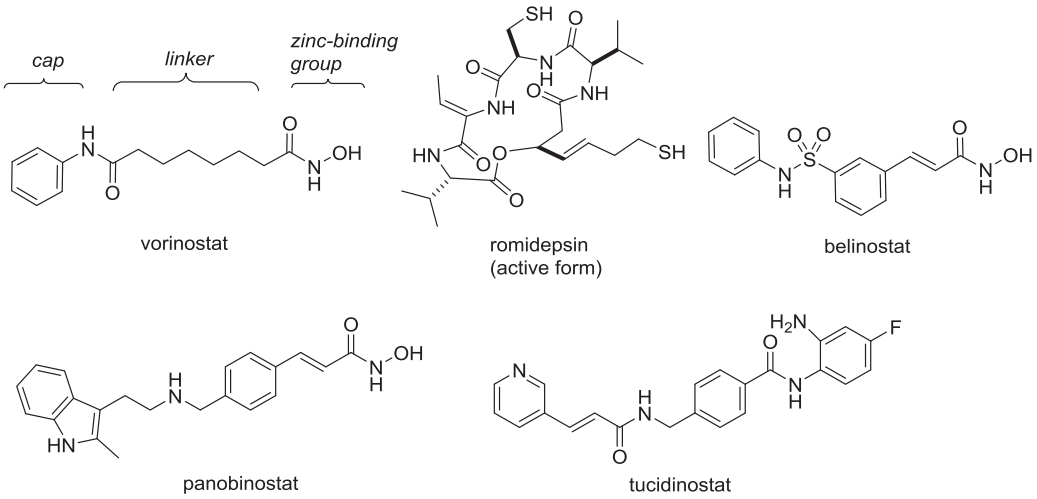

Figure 1. Approved HDAC inhibitors, with the common pharmacophore indicated for vorinostat.

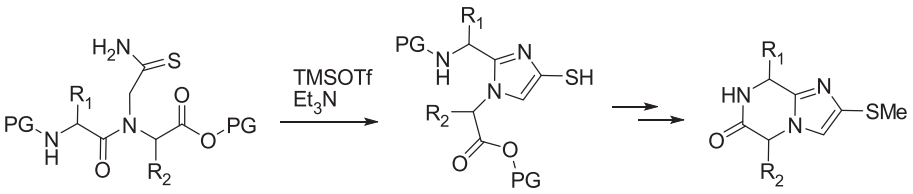

Figure 2. The Bischoff synthesis of an imidazo-ketopiperazine scaffold from a dipeptidyl thioamide.

inhibitor, the larger peptides exhibit varying degrees of isoform selectivity that may be important for the avoidance of side effects in therapeutic applications.

Our previous studies on the total synthesis of the romidepsin family of HDAC inhibitors and their structure–activity (SAR) relationships demonstrate that considerable structural variation of the scaffold is tolerated without compromising biological activity [11–17]. In this work, we ask the question whether high HDAC affinity and selectivity can be achieved within a smaller non-macrocyclic framework. We had several basic requirements in our search for a new scaffold: (i) reduction of molecular weight and H-bond donors and acceptors compared to the macrocycles to enhance cell permeability; (ii) retention of chirality to ensure a non-flat topology that can form isoform-selective interactions with the chiral enzyme rim; (iii) accessibility from commercial building blocks available with high diversity; and (iv) ability to introduce a hydroxamic acid to favour active site interactions with the zinc cation.

The above factors led us to consider an imidazo-ketopiperazine scaffold as a potential solution. This compact bicyclic heterocycle complies with guidelines for oral bioavailability while incorporating two chiral centres that originate from readily available amino acid starting materials. A further attractive feature was the resemblance to diketopiperazines, a privileged scaffold around which we have constructed compound libraries by solution and solid-phase synthesis [18–22]. The imidazo-ketopiperazine was first reported by Bischoff and coworkers, as part of their study on an imidazole *cis*-amide bond peptidomimetic [23]. The dipeptides **1** (figure 2) containing *N*-glycinyl thioamide substituents underwent dehydrative cyclization to the imidazole **2** under conditions similar to those developed by Hopkins [24]. In one example with L-Ala-L-Ala ($R_1 = R_2 = Me$), **2** was further cyclized to the imidazo-ketopiperazine **3**. We envisioned that an adaptation of this route by elongation of the thioalkyl group to incorporate a zinc-binding group would provide a template for HDAC inhibition with the imidazo-ketopiperazine core serving as the cap.

2. Methods

Detailed experimental procedures for compound synthesis and characterization data, protocols for biochemical HDAC enzyme assays and cell-based assays, and molecular docking are provided in the electronic supplementary material.

3. Results and discussion

Our first compounds featured the L-Phe-L-Ala version of **2**. In a telescoped one-pot sequence of three reactions (scheme 1), L-Ala methyl ester **4** was alkylated to give glycinyl amide **5** which was condensed with Cbz-L-Phe using propanephosphonic acid anhydride (T3P) as coupling agent to provide dipeptide **6**. In the same pot, the solvent was evaporated off and the residue redissolved in 1,2-dimethoxyethane followed by treatment with Lawesson's reagent to effect selective thionation. The product thioamide **7** was isolated in 89% overall yield over the three operations. The dehydrative cyclization of thioamide **7** with trimethylsilyl triflate afforded thiol **8**, which was conveniently stored as the disulfide **9** obtained by refluxing in toluene.

When desired, the thiol was regenerated from disulfide **9** by reduction and we then elaborated the compound to the imidazo-ketopiperazine by two sequences that differ in the order of the steps (scheme 2). In the first route, thiol **9** was alkylated with two ω-halo-esters, leading to the thioethers

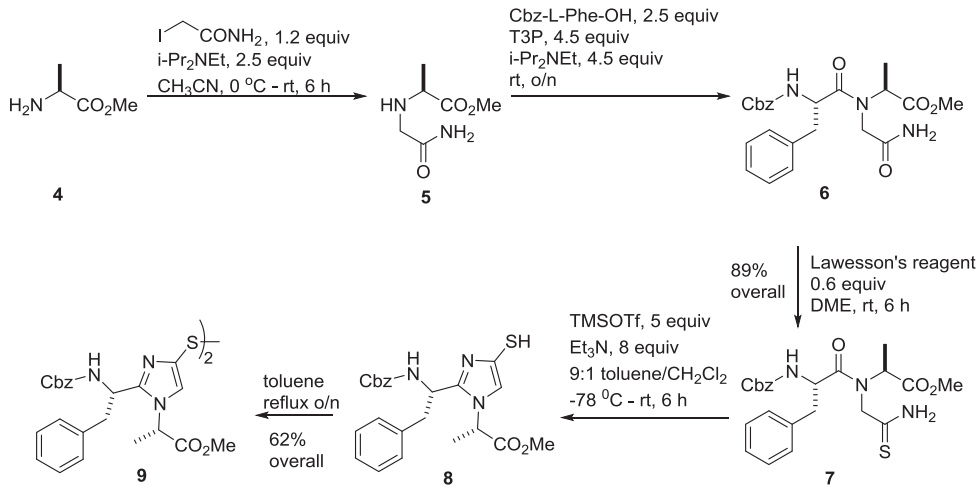

Scheme 1. Synthesis of the imidazolyl thiol **8** and the corresponding disulfide **9**.

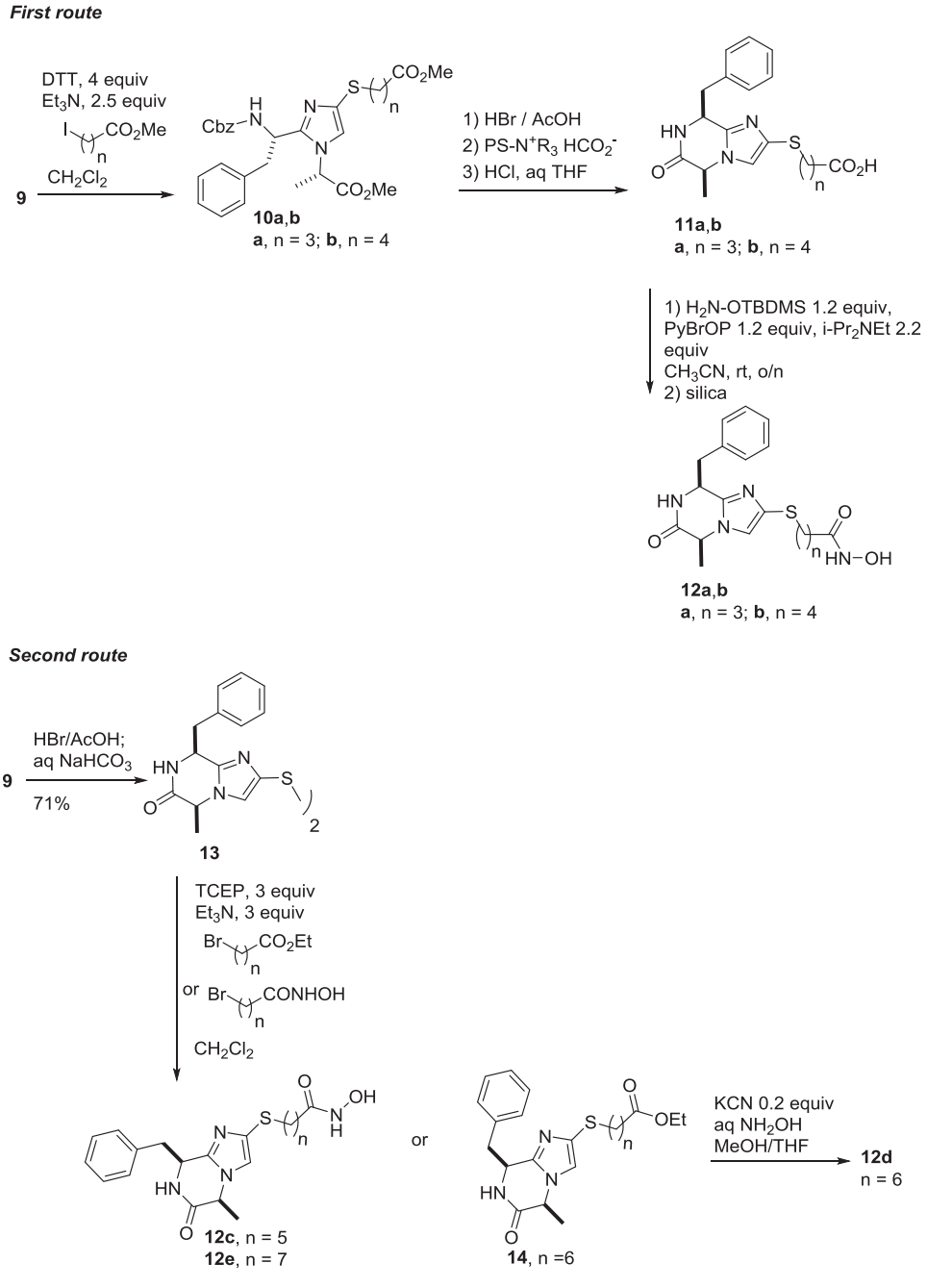

Scheme 2. Synthesis of hydroxamic acids **12a–e** from disulfide **9**.

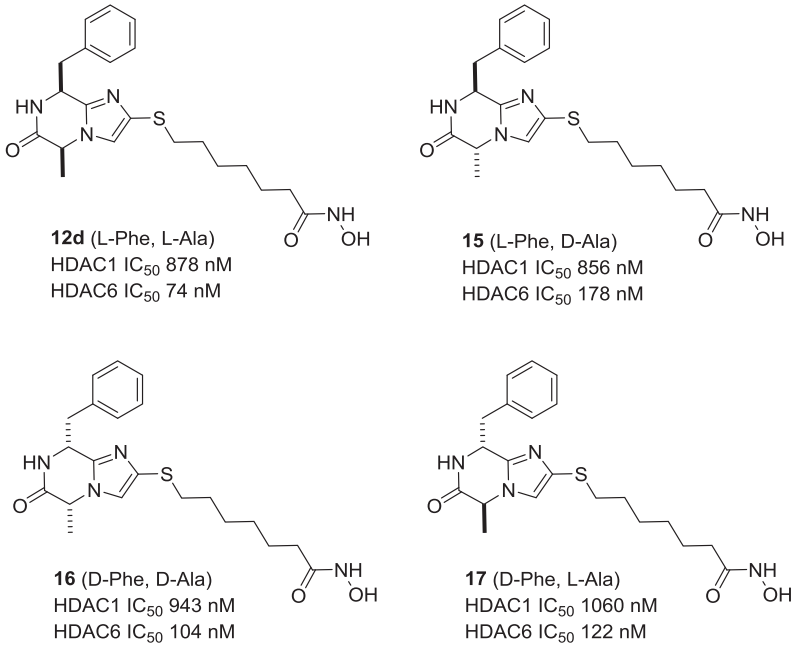

Figure 3. HDAC1 and HDAC6 inhibitory profile for the four diastereomers **12d**, **15**, **16** and **17**.

Table 1. Influence of linker length on inhibition of selected HDAC isoforms, data obtained from $n = 1$ experiments.

compound, linker length *n*	HDAC1 IC_{50} (μM)	HDAC6 IC_{50} (μM)	HDAC8 IC_{50} (μM)
12a, $n = 3$	24	4.6	3.4
12b, $n = 4$	3.6	0.9	
12c, $n = 5$	4.5	2.0	
12d, $n = 6$	0.9	0.1	0.1
12e, $n = 7$	0.8	0.3	2.8

10a and **10b**, varying in the length of the linker. Removal of the *N*-terminal Cbz protecting group gave the protonated amines, which were liberated to the free base by neutralization with a polystyrene-supported formate ion exchange resin. The free amine spontaneously cyclized to the imidazo-ketopiperazine and the sidechain ester was then hydrolyzed to afford the carboxylic acids **11a** and **11b**. A number of methods were investigated for the conversion of the carboxylic acid to the corresponding hydroxamic acid. The most reliable proved to be coupling with the protected *tert*-butyldimethylsilyl ether of hydroxylamine. Afterwards, the silyl ether was conveniently removed by stirring the crude reaction mixture with silica, thus avoiding the need for a separate deprotection step. By this method, we obtained hydroxamic acids **12a** and **12b** with linker lengths $n = 3$ and $n = 4$.

While the above route was also applicable to compounds with longer linker lengths, an alternative provided higher overall yields. In this sequence, the disulfide **9** was first cyclized to the imidazo-ketopiperazine **13**. The disulfide was reduced and directly alkylated with ω-halo-hydroxamic acids to give **12c** and **12e** with linker lenghts $n = 5$ and $n = 7$. For the hydroxamic acid **12d** with a linker length $n = 6$, alkylation with an ester afforded the intermediate **14**, which was converted to the hydroxamic acid by cyanide catalyzed nucleophilic displacement with hydroxylamine.

With the hydroxamic acids **12a–e** in hand, we were ready to evaluate whether the imidazo-ketopiperazine cap was compatible with HDAC inhibition. The initial profiling involved biochemical assays against two HDAC isoforms, the class I nuclear isoform HDAC1 and the class II cytoplasmic isoform HDAC6. We were pleased to find that all five compounds have micromolar or submicromolar IC_{50} values against these two isoforms (table 1). As expected from the SAR of other HDAC inhibitors, the activity is profoundly influenced by the linker and the optimum was reached with the longer six and seven carbon linkers present in **12d** and **12e**. These were additionally tested, together with **12a**, against HDAC8 and **12d** in particular exhibited submicromolar activity. Gratifyingly, the preliminary data suggested that selective inhibition of HDAC isoforms can be achieved with our chiral imidazo-ketopiperazine heterocyclic cap.

Since the imidazo-ketopiperazine scaffold contains two chiral centres, we were interested in the influence of stereochemistry on target affinity. Through a reaction sequence analogous to scheme 2, we carried out a stereochemical scan and prepared the three diastereomers **15–17** of hydroxamic acid **12d**. While all four compounds show similar levels of activity and isoform selectivity between HDAC1 and HDAC6 (figure 3), it is possible that replacement of the Phe and Ala sidechains by other residues may result in significant differences in bioactivity between diastereomers.

In order to have a more detailed picture of the isoform selectivity, we submitted hydroxamic acid **12d** for testing against all 11 human HDACs by the French CRO Cerep. At a test concentration of 10 μM, **12d** had a remarkable degree of isoform selectivity and significantly inhibited only three isoforms, *viz*. HDAC1, HDAC6 and HDAC8 (table 2). Between these three isoforms, the determination of IC_{50} values revealed **12d** to be most potent at HDAC6 inhibition, with a 13-fold degree of selectivity compared to HDAC8, the next highest inhibited isoform.

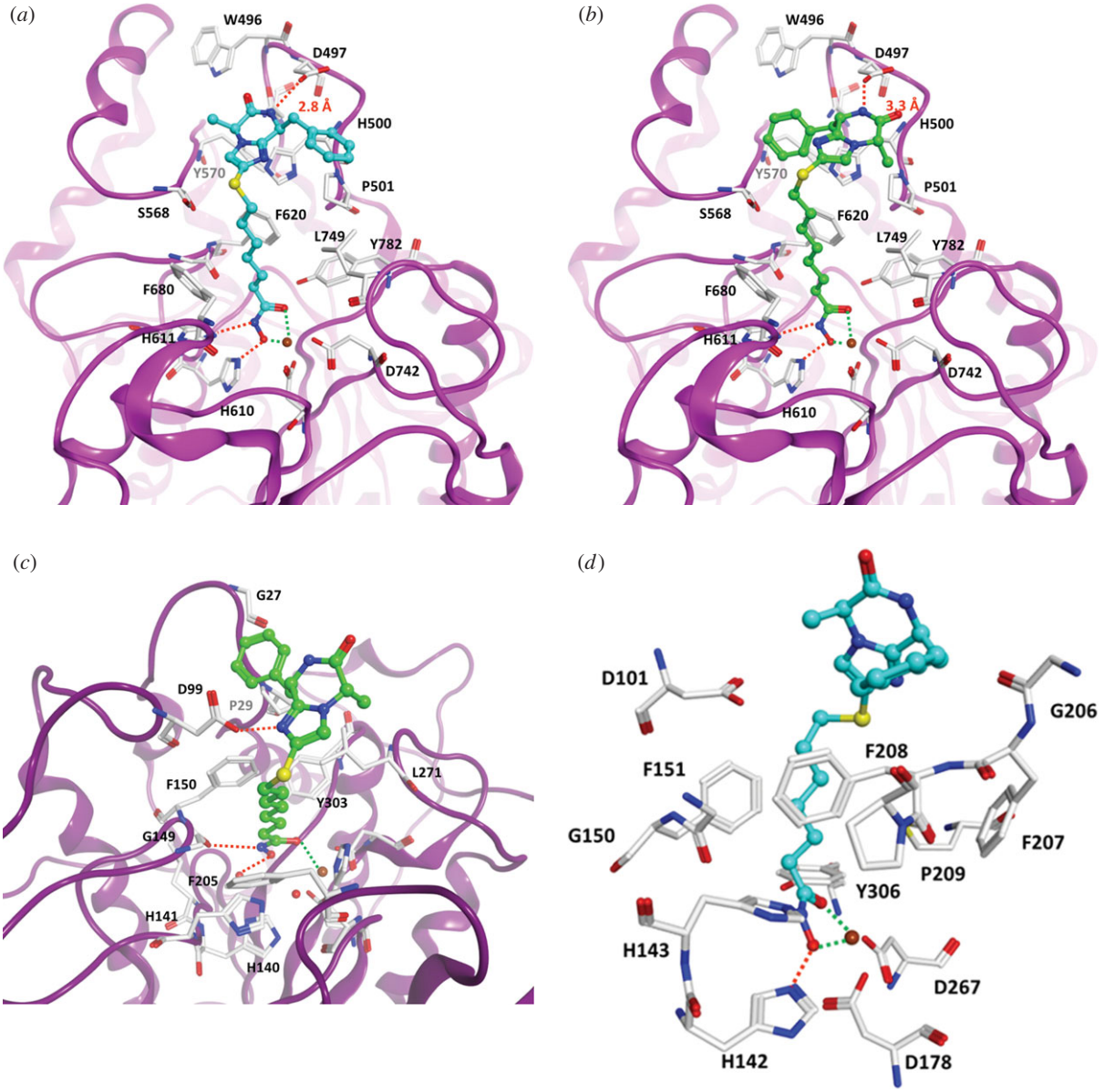

Figure 4. Molecular docking of compounds (*a*) **12d** and (*b*) **12e** in the HDAC6 active site (PDB ID 5EDU). For comparison, the docking (*c*) of **12e** in the HDAC1 active site (PDB 5ICN) and (*d*) of **12d** in the HDAC8 active site (PDB ID 2V5X) is shown. Hydrogen bonds are shown as orange coloured dashed lines, coordination between the hydroxamic acid and the zinc ion (coloured brown) is shown as green coloured dashed lines. Conserved water molecules in the active site are shown as red spheres.

Table 2. Percentage inhibition of individual HDAC isoforms by **12d**, values are the mean of two measurements. IC_{50} values were determined for HDAC1, HDAC6 and HDAC8. Owing to differences in assay conditions, absolute values are not directly comparable with table 1.

class I isoforms		class IIa isoforms		class IIb and IV isoforms	
HDAC1	57%, IC_{50} 7.3 µM	HDAC4	4%	HDAC6	99%, IC_{50} 160 nM
HDAC2	32%	HDAC5	23%	HDAC10	44%
HDAC3	38%	HDAC7	9%	HDAC11	10%
HDAC8	90%, IC_{50} 2.1 µM	HDAC9	1%		

The observed selectivity for the three HDAC isoforms was modelled by docking the inhibitors into the enzyme active site. Bidentate chelation of the hydroxamic acid was observed for HDAC6 as well as HDAC8, as illustrated for compounds **12d** and **12e** (figure 4*a*,*b*). In addition, a hydrogen bond is predicted between the imidazo-ketopiperazine and the acidic D497 residue for the compounds with linker lengths of $n = 6$ and $n = 7$. Interestingly, the orientation of binding is 'flipped' between **12d** and **12e** with respect to the positioning of the phenyl and methyl groups. The availability of two binding modes may explain the relatively low differences in activity between the four diastereomers (figure 3). In the case of **12d**, the terminal benzyl group attached to the imidazo-ketopiperazine is accommodated in the hydrophobic pocket formed between P501 and L749 (figure 4*a*). On the other hand, a weaker binding was

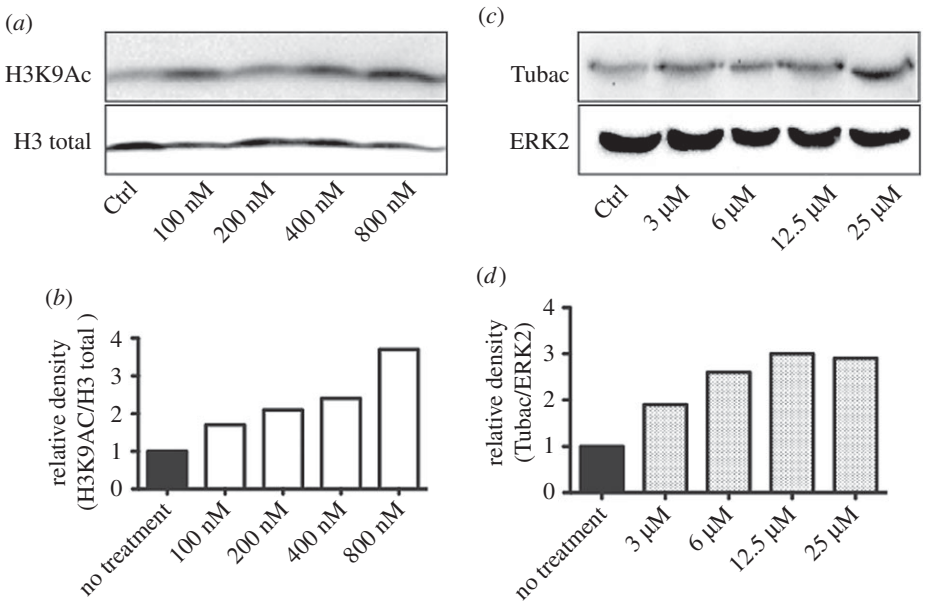

Figure 5. Western blot analysis of (*a*) acetylated histone H3K9 and (*b*) acetylated tubulin and their relative loading controls (H3 total and ERK2), after treatment of U937 cells with HDAC inhibitor **12e**. Western blot signals were quantified by densitometry using Image Lab 6.0 (BIORAD) and signal intensities plotted against the loading controls (*b*,*d*).

Table 3. Cell growth inhibition by compounds **12c**–**e** in MV4-11, THP-1 and U937 cell lines.

compound	cell line	IC_{50} (µM, $n = 3$), 72 h	IC_{50} (µM, $n = 3$) 96 h
12c	MV4-11	>25	>25
	THP-1	>25	>25
	U937	>25	>25
12d	MV4-11	4.5 ± 0.3	6.8 ± 0.4
	THP-1	10.4 ± 0.3	9.0 ± 0.3
	U937	0.9 ± 0.2	0.5 ± 0.7
12e	MV4-11	1.7 ± 0.2	2.6 ± 0.7
	THP-1	1.7 ± 0.2	1.7 ± 0.6
	U937	0.1 ± 0.02	0.3 ± 0.2

predicted for HDAC1, with monodentate coordination of the hydroxamic acid (figure 4*c*), and is consistent with the experimentally observed reduced activity against this isoform. In the case of HDAC8, **12d** is more solvent exposed and sticking out of the enzyme pocket, with the benzyl side-chain of the scaffold in interaction with F208 (figure 4*d*).

We profiled compounds **12c**–**e** with the longer linkers in cellular assays for the growth inhibition of cancer cell lines. While compound **12c** with the linker length $n = 5$ was relatively inactive (table 3), both **12d** and **12e** with linker lengths of $n = 6$ and $n = 7$ were micromolar inhibitors and the U937 lymphoma cell line was particularly sensitive to these compounds. Compound **12e** was more active than **12d**, and we believe this might be due to an increased lipophilicity affecting cellular uptake and efflux rather than intrinsic target affinity. Western blotting of U937 cell extracts treated with **12e** demonstrated a dose-dependent increase in histone H3 and tubulin acetylation levels (figure 5), suggesting target engagement with both class I and class II HDAC isoforms. Given the activity profile (table 1), we believe the cellular effects are primarily due to the inhibition of the nuclear HDAC1 and HDAC8 as well as the cytoplasmic HDAC6.

4. Conclusion

We report the imidazo-ketopiperazine scaffold as a new 'cap' for the assembly of potent and isoform-selective HDAC inhibitors. The scaffold contains two chiral centres and is readily accessible from amino acid precursors. Evaluation of the compounds revealed **12d** and **12e** to be submicromolar inhibitors of HDAC6, and a docking model is proposed for the binding interactions between these compounds and HDAC6, HDAC8 and HDAC1. In the case of **12d**, screening against the full panel of HDACs revealed HDAC6 selectivity of at least 10-fold over all other isoforms. In cell-based assays, the compounds were micromolar inhibitors of cancer cell lines and **12e** displayed a dose-dependent increase in histone and tubulin acetylation levels. Further analogues in this series are currently under investigation.

Data accessibility. Details for all experimental procedures have been uploaded as part of the electronic supplementary material.

Authors' contributions. B.L. and R.N. carried out the compound synthesis, under the supervision of L.B. and A.G., respectively. J.S. and A.C. assayed compounds against HDAC1, HDAC6 and HDAC8 under the supervision of M.J., with HDAC8 provided by M.M. and C.R. J.M. conducted the molecular docking under the supervision of W.S. Cellular assays were performed by M.T.B. The project was conceived and designed by L.B. and A.G. All authors contributed to the analysis and interpretation of data, drafting the article, revision and final approval of the version to be published.

Competing interests. We declare we have no competing interests.

Funding. We gratefully acknowledge funding from the following sources: B.L. and L.B. (Rouen) were funded by the INTERREG ISCE:-Chem (Ref: 1917/4061) selected under the European Cross-border Cooperation Programme INTERREG IV A France (Channel)—England, co-funded by the ERDF and the Centre Universitaire Normand de Chimie Organique 'Crunch' network. R.N. and A.G. (Norwich) were funded by the European Union's Seventh

Framework Programme for Research, Technological Development and Demonstration under Grant Agreement 602080 (A-ParaDDisE) and the University of East Anglia. M.T.B. (Marseille) was funded by La Ligue Contre le Cancer and the Institut National de la Santé et de la Recherche Médicale (INSERM). J.S., A.C. and M.J. (Freiburg) were funded by the European Union's Seventh Framework Programme for Research, Technological Development and Demonstration under Grant Agreement 241865 (SEtTReND) and 602080 (A-ParaDDisE), and the Deutsche Forschungsgemeinschaft (DFG, Ju295/13-1). M.M. and C.R. (Strasbourg) were funded by the European Union's Seventh Framework Programme for Research, Technological Development and Demonstration under Grant Agreement 241865 (SEtTReND) and 602080 (A-ParaDDisE), and the Centre National de la Recherche Scientifique (CNRS), the Institut National de la Santé et de la Recherche Médicale (INSERM) and the Université de Strasbourg. J.M. and W.S. (Halle) were funded by the European Union's Seventh Framework Programme for Research, Technological Development and Demonstration under Grant Agreement 241865 (SEtTReND) and 602080 (A-ParaDDisE), and the Deutsche Forschungsgemeinschaft (DFG, Si868/13-1). A.G., M.J., W.S and M.T.B. are members of the COST Action CM1406 'Epigenetic Chemical Biology' and acknowledge financial support from the network.

References

1. Zwergel C, Stazi G, Valente S, Mai A. 2016 Histone deacetylase inhibitors: updated studies in various epigenetic-related diseases. *J. Clin. Epigenet.* **2**, 1–7.
2. Manal M, Chandrasekar MJN, Priya JG, Nanjan MJ. 2016 Inhibitors of histone deacetylase as antitumor agents: a critical review. *Bioorg. Chem.* **67**, 18–42. (doi:10.1016/j.bioorg.2016.05.005)
3. Roche J, Bertrand P. 2016 Inside HDACs with more selective HDAC inhibitors. *Eur. J. Med. Chem.* **121**, 451–483. (doi:10.1016/j.ejmech.2016.05.047)
4. Shen S, Kozikowski AP. 2016 Why hydroxamates may not be the best histone deacetylase inhibitors—what some may have forgotten or would rather forget? *ChemMedChem* **11**, 15–21. (doi:10.1002/cmdc.201500486)
5. Kawai K, Nagata N. 2012 Metal–ligand interactions: an analysis of zinc binding groups using the Protein Data Bank. *Eur. J. Med. Chem.* **51**, 271–276. (doi:10.1016/j.ejmech.2012.02.028)
6. Nakao Y *et al.* 2006 Azumamides A-E: histone deacetylase inhibitory cyclic tetrapeptides from the marine sponge *Mycale izuensis*. *Angew. Chem. Int. Ed. Engl.* **45**, 7553–7557. (doi:10.1002/anie.200602047)
7. Wen S, Carey KL, Nakao Y, Fusetani N, Packham G, Ganesan A. 2007 Total synthesis of azumamide A and azumamide E, evaluation as histone deacetylase inhibitors, and design of a more potent analogue. *Org. Lett.* **9**, 1105–1108. (doi:10.1021/ol070046y)
8. Maolanon AR, Kristensen HM, Leman LJ, Ghadiri MR, Olsen CA. 2017 Natural and synthetic macrocyclic inhibitors of the histone deacetylase enzymes. *Chembiochem* **18**, 5–49. (doi:10.1002/cbic.201600519)
9. Ganesan A. 2016 Romidepsin and the zinc-binding thiol family of natural product HDAC inhibitors. In *Successful drug discovery*, vol. 2 (eds J Fischer, WE Childers), pp. 13–30. Weinheim, Germany: Wiley.
10. Ganesan A. 2015 Macrocyclic inhibitors of zinc-dependent histone deacetylases (HDACs). In *Macrocycles in drug discovery* (ed. J Levin), pp. 109–140. Cambridge, UK: RSC.
11. Yurek-George A, Habens F, Brimmell, M, Packham G, Ganesan A. 2004 Total synthesis of spiruchostatin A, a potent histone deacetylase inhibitor. *J. Am. Chem. Soc.* **126**, 1030–1031. (doi:10.1021/ja039258q)
12. Doi T, Iijima Y, Shin-ya K, Ganesan A, Takahashi T. 2006 A total synthesis of spiruchostatin A. *Tetrahedron Lett.* **47**, 1177–1180. (doi:10.1016/j.tetlet.2005.12.031)
13. Yurek-George A *et al.* 2007 The first biologically active synthetic analogues of FK228, the depsipeptide histone deacetylase inhibitor. *J. Med. Chem.* **50**, 5720–5726. (doi:10.1021/jm0703800)
14. Wen S, Packham G, Ganesan A. 2008 Macrolactamization versus macrolactonization: a practical total synthesis of FK228, the depsipeptide histone deacetylase inhibitor. *J. Org. Chem.* **73**, 9353–9361. (doi:10.1021/jo801866z)
15. Iijima Y, Munakata A, Shin-ya K, Ganesan A, Doi T, Takahashi T. 2009 A solid-phase total synthesis of the cyclic depsipeptide HDAC inhibitor spiruchostatin A. *Tetrahedron Lett.* **50**, 2970–2972. (doi:10.1016/j.tetlet.2009.04.005)
16. Benelkebir H, Marie S, Hayden A, Lyle J, Loadman P, Crabb SJ, Packham G, Ganesan A. 2011 Total synthesis of largazole and analogues: HDAC inhibition, antiproliferative activity and metabolic stability. *Bioorg. Med. Chem.* **19**, 3650–3658. (doi:10.1016/j.bmc.2011.02.024)
17. Benelkebir H, Donlevy AM, Packham G, Ganesan A. 2011 Total synthesis and stereochemical assignment of burkholdac B, a depsipeptide HDAC inhibitor. *Org. Lett.* **13**, 6334–6337. (doi:10.1021/ol202197q)
18. Wang H, Usui T, Osada H, Ganesan A. 1999 Synthesis and evaluation of tryprostatin B and demethoxyfumitremorgin C analogues. *J. Med. Chem.* **43**, 1577–1585. (doi:10.1021/jm9905662)
19. Wang H, Ganesan A. 2000 The *N*-acyliminium Pictet-Spengler condensation as a multicomponent combinatorial reaction on solid phase and its application to the synthesis of demethoxyfumitremorgin C analogues. *Org. Lett.* **1**, 1647–1649. (doi:10.1021/ol991030d)
20. Bonnet D, Ganesan A. 2002 Solid-phase synthesis of tetrahydro-β-carboline-hydantoins via the *N*-acyliminium Pictet-Spengler reaction and cyclative cleavage. *J. Comb. Chem.* **4**, 546–548. (doi:10.1021/cc020026h)
21. Bonnet D, Margathe JF, Radford S, Pflimlin E, Riche S, Doman P, Hibert M, Ganesan A. 2012 Combinatorial aid for underprivileged scaffolds: solution and solid-phase strategies for a rapid and efficient access to novel aza-diketopiperazines (Aza-DKP). *ACS Comb. Sci.* **14**, 323–334. (doi:10.1021/co300015k)
22. Regenass P, Bosc D, Riché S, Gizzi P, Hibert M, Karmazin L, Ganesan A, Bonnet D. 2017 Comparative study of the synthesis and structural and physicochemical properties of diketopiperazines vs aza-diketopiperazines. *J. Org. Chem.* **82**, 3239–3244. (doi:10.1021/acs.joc.6b02895)
23. Petit S, Fruit C, Bischoff L. 2010 New family of peptidomimetics based on the imidazole motif. *Org. Lett.* **12**, 4928–4931. (doi:10.1021/ol102118u)
24. Holler T, Ruan F, Spaltenstein A, Hopkins PB. 1989 Total synthesis of marine mercaptohistidines: ovothiols A, B, and C. *J. Org. Chem.* **54**, 4570–4575. (doi:10.1021/jo00280a022)